- Technical paper -

EFFECTS OF STONE POWDER SLUDGE ON THE STRENGTH AND MICROSTRUCTURE OF ALKALI-ACTIVATED FLY ASH PASTES

Sejin CHOI[*1]・Paulo J MONTEIRO[*2]・Moohan KIM[*3]

ABSTRACT

Stone powder sludge is a by-product by manufacturing of crushed sand, most of this is dumped in landfills and it is a major environmental issue. This paper investigates the effects of stone powder sludge on the strength and microstructure of alkali-activated fly ash pastes. Stone powder sludge produced from crushed aggregate factory was used to replace fly ash at replacement ratios of 0%, 10%, 20% and 30% by mass. Unit weight and compressive strength of the samples were measured, and scanning electron microscope/ energy dispersive spectroscopy (SEM/EDS) analysis and X-ray diffraction (XRD) were performed.

Key words: stone powder sludge, alkali-activated fly ash, compressive strength, microstructure

1. INTRODUCTION

Recently, the usage rate of the crushed sand for concrete has been increased due to the exhaustion of good natural aggregates. In 2004, the usage rate of crushed sand in Korea was about 28% [1]. Stone powder sludge is a by-product of the manufacturing process of crushed sand and is collected by a filter press from the washed sludge water where water is used to clean the powder of crushed sand. The water content in stone powder sludge ranges from 20% to 50% by weight, and due to this it is difficult to handle, transport and recycle stone powder sludge. The quantity of stone powder sludge produced from crushed aggregate factories in Korea is approximately 7.5 million tons each year. Most of this is dumped with soil in landfills. The disposal of stone powder sludge is a major environmental issue. Hence, there is great need to investigate solutions on how to utilize a by-product like stone powder sludge more efficiently.

Stone powder sludge usually consists of SiO_2 and Al_2O_3 similar to Class F fly ash [2], which can be used in geopolymer as a raw material. It is known that the reaction of solid aluminosilicate with a highly concentrated aqueous alkali hydroxide or silicate solution produces a synthetic alkali aluminosilicate material generically called 'geopolymer' [3]. This material can provide comparable performance to traditional cementitious binders in a range of applications, but with the added advantage of significantly reduced Greenhouse emissions [4] because cement manufacture generates carbon dioxide (CO_2) emissions from calcination of limestone in the raw materials, and from fuel combustion at the rate of approximately 1 ton of CO_2 per ton of cement [5, 6]. In addition, geopolymer could be made predominantly from industrial waste materials such as fly ash, granulated blast furnace slag and mine tailings, which can provide a replacement for the silicates concentrations required for matrix formation of geopolymer [7]. While the strength development of pozzolanic cements generally depends on the presence of calcium, geopolymer does not utilize the formation of calcium-silicate-hydrates (CSH) for matrix formation and strength [8]. In addition, microstructure and physical, mechanical, chemical and thermal properties of geopolymer vary to a large extent depending predominantly on the raw material from which they are

*1 Principal Researcher, SAMPYO R&D Center, Korea, Dr.E., JCI Member

*2 Professor, Civil and Environmental Engineering, University of California at Berkeley, U.S. Dr.E., ACI Member

*3 Professor, Architectural Engineering, Chungnam National University, Korea, Dr.E., JCI Member

derived [9].

During the last few years, some researchers have studied the use of stone powder sludge in the cement and concrete industries. However, they performed their experiment with dried stone powder, and it was not practical methods to efficiently use the stone powder sludge in concrete industry. Because the material has some water content originally, it needs high energy consumption and cost to dry the material.

In this study, we examined the strength and microstructure of alkali-activated fly ash pastes using stone powder sludge that had some water content without the drying. The objective of this research was to compare and analyze the strength property and microstructure of alkali activated fly ash pastes when using different replacement ratios of stone powder sludge.

2. EXPERIMENTAL PROCEDURE

2.1 Materials

Class F fly ash obtained from the thermal power plant at Dangjin in Korea was used. The stone powder sludge used in this investigation was granite sludge that had some water content of 20.7%, from Sampyo Aggregate Co. in Korea. **Fig. 1** (small picture) shows the stone powder sludge that had some water.

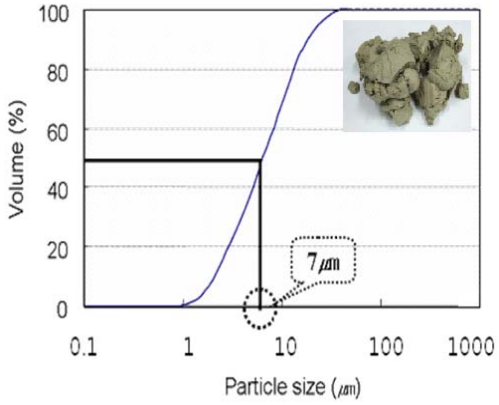

Fig. 1 Grading curve of stone powder sludge

Table 1 Chemical composition of fly ash and stone powder sludge (%)

Materials	SiO_2	Al_2O_3	Fe_2O_3	K_2O	CaO	MgO	Na_2O
Fly ash	56.07	27.18	5.48	1.25	3.46	0.01	0.05
SPS[1)]	62.11	15.72	4.08	4.98	3.02	2.25	2.64

1) Stone powder sludge (oven dried condition)

The grading of the stone powder sludge was measured by using a Laser diffraction particle size analyzer. As shown in **Fig. 1**, the particle size of the stone powder sludge ranged from 0.92 ㎛ to 46.08 ㎛. The average size was about 7 ㎛. The densities of fly ash and stone powder sludge were 2.25 and 1.95 (oven dried condition), respectively. The chemical compositions of fly ash and stone powder sludge are shown in **Table 1**. The sodium silicate solution (Na_2SiO_3) of 1.36 g/cm^3 density with Ms (modulus) = 3.12 (Na_2O = 8.2% and SiO_2 = 26.4%) was supplied by PQ USA. Sodium hydroxide solution (NaOH) of 10M (molarity) was supplied by Fisher Scientific USA. Na_2SiO_3 and NaOH solutions were used for the activation of fly ash and blast furnace slag mixes.

2.2 Method

Stone powder sludge was used to replace fly ash at replacement ratios of 0%, 10%, 20%, 30%, 50%, and 100% by weight. The solution/solid (fly ash and stone powder sludge) ratio was 0.2 (S100 mixes), 0.3 (S50 mixes), and 0.5 (F100, F90, F80, F70 mixes). The mix proportions are given in **Table 2**. Fly ash and stone powder sludge were mixed with the alkaline solution and then cast into 25.4×25.4 mm cylinder shaped moulds. A total of 3 samples were prepared for every mix. All specimens were cured at 80℃ for 24 hours in chamber. They were then kept at a room temperature of about 23℃ until the mechanical test such as unit weight and compressive strength.

Table 2 Mixture proportions and test items

Mix	S/(f+s)[1)] (%)	FA (%)	SPS (%)	NaOH (mole)	Na_2SiO_3/NaOH (%)	Test items
S100-0.5	0.2	0	100	10	0.5	Compressive
S100-1.5	0.2	0	100	10	1.5	Strength
S100-2.5	0.2	0	100	10	2.5	Unit
S50-0.5	0.3	50	50	10	0.5	weight[2)]
S50-1.0	0.3	50	50	10	1.0	SEM/EDS[2)]
S50-1.5	0.3	50	50	10	1.5	XRD[2)]
F100-1.5	0.5	100	0	10	1.5	
F90-1.5	0.5	90	10	10	1.5	
F80-1.5	0.5	80	20	10	1.5	
F70-1.5	0.5	70	30	10	1.5	

1) Solution/(fly ash + stone powder sludge) ratio
2) For F100, F90, F80 and F70 mixes

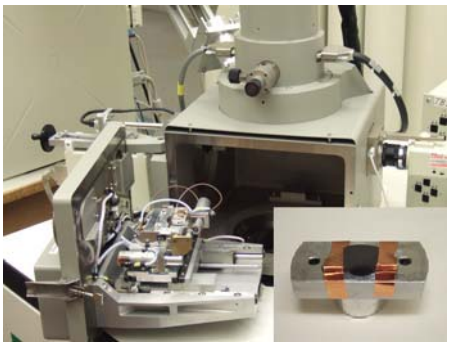

Fig. 2 Test machine and sample for SEM/EDS analysis

Fig. 3 Test machine and sample for XRD analysis

The specimens were micro structurally studied by LEO 430 scanning electron microscope/energy dispersive spectroscopy (SEM/EDS) (**Fig. 2**) and X-ray diffraction (XRD) (**Fig. 3**). The SEM/EDS analysis utilized secondary electron imaging of a cross section of test samples, which were coated with a thin film of gold before the SEM observation.

After the specimens were mechanically tested, some samples (F100 and F70 mix samples) were finely grounded to powder. X-ray powder diffraction patterns were obtained using a PANalytical X'Pert PRO MPD diffractometer with CoKα (λ= 1.790Å) radiation. The X-ray was generated at an acceleration voltage of 40kV and a filament emission of 40mA. The radius of goniometer was 240.00 mm. The samples were scanned from 3.016 º to 99.984º (2θ) with a step size of 0.0170º and scan step time of 20.027s.

3. RESULTS AND DISCUSSION

3.1 Compressive strength and unit weight

1) S100 and S50 mixes

The test results of compressive strength are given in **Table 3** and shown in **Fig. 4**. **Fig. 4** shows the variation of compressive strength with Na_2SiO_3/NaOH ratios. From the test results, it can be seen that the compressive strength of S100-1.5 (**Fig. 4** (a)) and S50-1.5 (**Fig. 4** (b)) mix with Na_2SiO_3/NaOH ratio 1.5 was higher than any other mixes in S100 and S50 mixes. In addition, the compressive strength of S50 mixes was higher than that of S100 mixes.

Table 3 Test results

Mix	Unit weight (g/cm^3)	Compressive strength (MPa)		
	28d	3d	7d	28d
S100-0.5			1.05	
S100-1.5			1.32	
S100-2.5			0.57	
S50-0.5	1.588[1)]		3.29	
S50-1.0	1.601[1)]		3.42	
S50-1.5	1.624[1)]		4.99	
F100-1.5	1.480	23.06	25.69	36.17
F90-1.5	1.444	16.31	17.23	30.52
F80-1.5	1.410	8.65	10.69	19.88
F70-1.5	1.389	5.41	5.88	16.52

1) Measured at 7 days

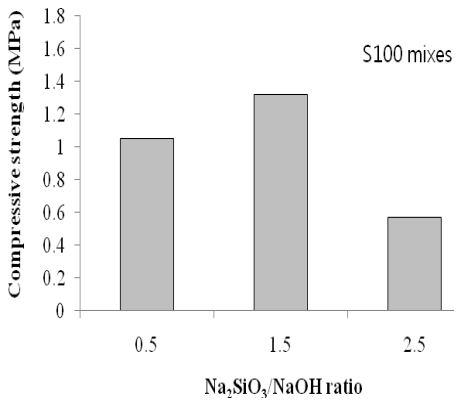

(a) S100 mixes

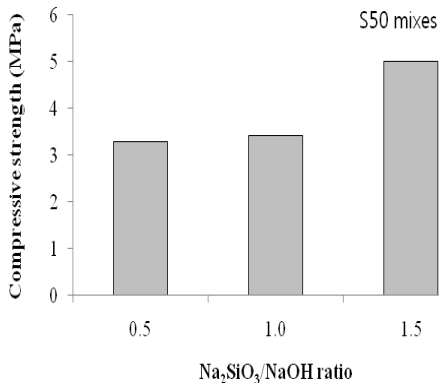

(b) S50 mixes

Fig. 4 Compressive strength versus Na_2SiO_3/NaOH ratios (7 days)

For S100 mixes, the compressive strength of the samples was low and it ranged from 0.57 to 1.05 MPa. This low development in compressive strength of S100 mixes may be because the alkali-activation degree of S100 mixes with only stone powder sludge without fly ash was very low. For S50 mixes, the compressive strength of the samples ranged from 3.29 to 4.99 MPa.

2) F100, F90, F80 and F70 mixes

Compressive strength of F100, F90, F80 and F70 alkali-activated fly ash mixes was determined at 3, 7 and 28 days. The test results of unit weight and compressive strength are given in **Table 3** and shown in **Fig. 5** and **6**, respectively. **Fig. 5** shows the variation of unit weight with stone powder sludge percentages. **Fig. 6** shows the variation of compressive strength with stone powder sludge percentages at different ages. From the test results, the incorporation of stone powder sludge reduced the unit weight of alkali-activated fly ash mixes.

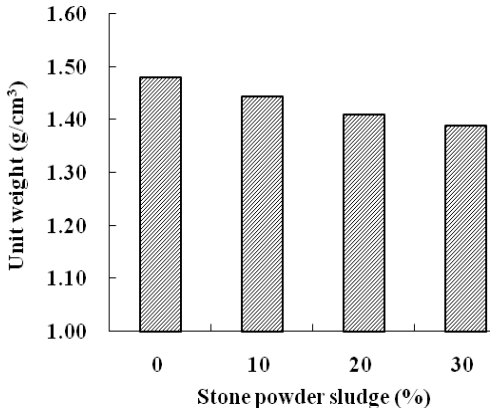

Fig. 5 Unit weight versus stone powder sludge (28 days)

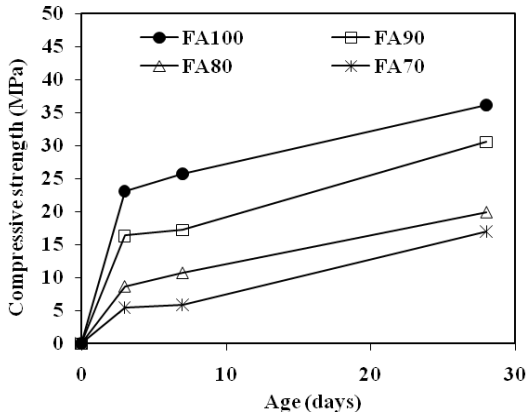

Fig. 6 Compressive strength versus age

The higher the replacement amount of stone powder sludge in alkali-activated fly ash mixes, the higher the reduction in unit weight of alkali-activated fly ash mixes. This is believed to be because the density of stone powder sludge (1.95) was lower than that of fly ash (2.25).

The compressive strength of FA90, FA80 and FA70 alkali-activated fly ash mixes with 10%, 20% and 30% fly ash replacement with stone powder sludge was lower than that of the alkali-activated fly ash control mix (FA100). The compressive strength of alkali-activated fly ash mixes decreased with an increase in the replacement ratio of stone powder sludge. In addition, the decreased degree of compressive strength increased as the replacement ratio of stone powder sludge was over 20 percentage. However, it is evident that the compressive strength continued to increase with the increase in age as shown in **Fig. 6**. At 28 days, the compressive strength of FA100 sample was 36.17 MPa. The compressive strength of alkali-activated fly ash mixes with stone powder sludge ranged from 16.52 to 30.52 MPa at 28 days.

3.2 SEM/EDS analysis

The microstructures and the semi-quantitative compositions of samples were studied using a scanning electron microscope (SEM) with energy dispersive spectroscopy (EDS).

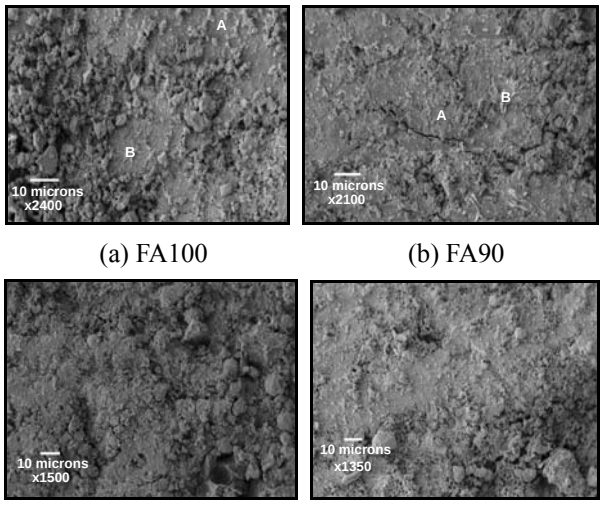

(a) FA100 (b) FA90

(c) FA80 (d) FA70

Fig. 7 SEM images of alkali-activated fly ash sample

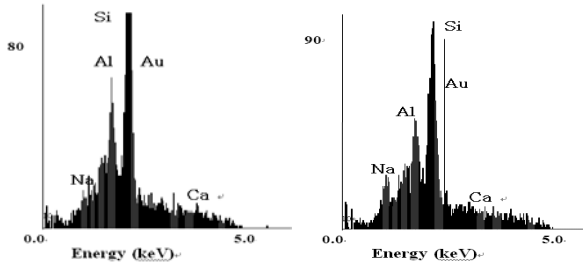

(point A) (point B)

(a) FA100

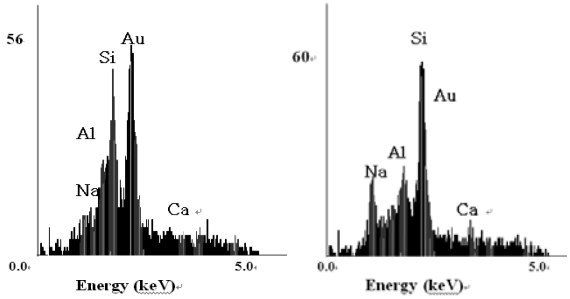

(point A) (point B)

(b) FA90

Fig. 8 EDS analysis of products in sample FA100 and FA90

The test results are shown in **Fig. 7** and **8**, respectively. **Fig. 7** shows the SEM micrographs of a cross section of F100, F90, F80 and F70 alkali-activated fly ash mixes. **Fig. 8** shows the EDS analysis of products in FA100 and FA90 alkali-activated fly ash samples. From the test results, small agglomerates and needle-shaped products on the surface of alkali-activated fly ash samples are observed (**Fig. 7**). In addition, the non-reacted fly ash particles are embedded into the matrix. **Fig. 8** shows products marked by A and B in **Fig. 7**, which are reaction products from fly ash and stone powder sludge (Si, Al and a small amount of Na). The EDS patterns of needle-shaped products (point B) are similar to that of the sample surface (point A).

3.4 X-ray diffraction

The test results are given in **Fig. 9**, which presents the XRD patterns of F100 and F70 alkali-activated fly ash samples indicating the identified phases. For all XRD diagrams, the broad and diffuse peaks are shown around 2θ=35º, implying amorphous or short-ordering structure phases generally emerged in

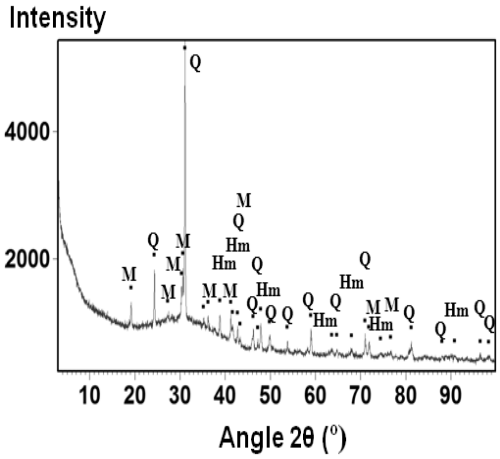

(a) FA100

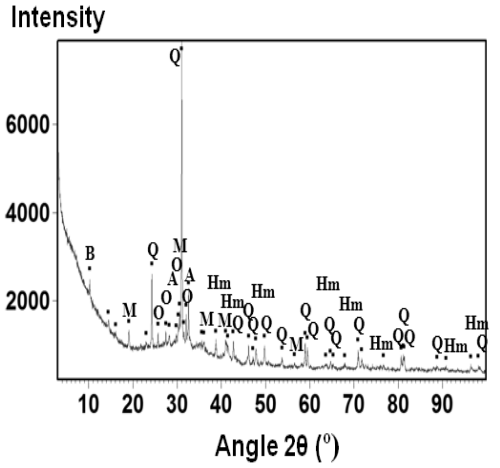

(b) FA70

Fig. 9 XRD patterns of FA100 and FA70 samples (B: biotite, Q: quartz, M: mullite, Hm: Hematite)

geopolymer. According to the X-ray data, the material obtained when the fly ash was activated with solutions of alkali hydroxide mixed with sodium silicate (F100) does not contain any crystalline phase except the ones existing in the fly ash (quartz, mullite, and hematite). However, the material obtained when the fly ash and stone powder sludge were activated with alkali solutions (F70) also contains some biotite, which may be attributed to the difference of chemical composition (MgO) between the fly ash and stone powder sludge. Except that, there are no newly emerged peaks compared with raw materials (fly ash and stone powder sludge). Thus, the reduction of compressive strength as we replaced a part of fly ash with stone powder sludge may be not due to final products' mineralogical differences.

4. CONCLUSIONS

(1) The higher the replacement ratio of stone powder sludge, the higher the reduction in unit weight of alkali-activated fly ash mixes.

(2) The compressive strength of S50 mixes was higher than that of S100 mixes. At the Na_2SiO_3/NaOH ratio of 1.5, the strength of the mix was higher than that of any other mixes with diffrent Na_2SiO_3/NaOH ratios.

(3) The compressive strength of alkali-activated fly ash mixes with stone powder sludge decreased as the replacement ratio of stone powder sludge increased. However, the compressive strength of all alkali-activated fly ash mixes continued to increase with the increase in age.

(4) The small agglomerates and needle-shaped products on the surface of alkali-activated fly ash samples were observed. The EDS analysis of the sample surface showed the presence of Si, Al and some Na.

(5) For XRD diagrams, F70 sample contained not only the ones existing in the fly ash, but also some biotite, which may be attributed to the difference of chemical composition (MgO) between the fly ash and stone powder sludge.

REFERENCES

[1] SJ. Choi et al: Influence of W/B ratio and replacement ratio of crushed sand on the fluidity and compressive strength of high strength concrete, K/J construction material symp., Vol.8, 2006, pp.153-158

[2] JM. Kim et al: The density and strength properties of lightweight foamed concrete using stone-powder sludge in hydrothermal reaction condition, J of the Korea Concrete Institute, Vol.18, 2006, pp.687-693

[3] J. Davidovits: Geopolymers: Inorganic Polymeric New Materials, J of thermal analysis, Vol.37, 1989, p.1633

[4] E. Gartner: Industrially interesting approaches to "low-CO_2" cements, Cement and Concrete Research, Vol.34, 2004, pp.1489-1498

[5] D. Carroll et al: U.S. Portland cement industry, concrete and global climate, Proceed. of the 1998 91st Annual Meeting and Exhibition, 1998, pp.9

[6] Xu A In: Chandra S (ed) Waste materials used in concrete manufacturing, Noyes Publications, 1997, pp.141-173

[7] M. Sofi et al: Bond performance of reinforcing bars in inorganic polymer concrete (IPC), J Mater Sci., Vol.42, 2007, pp.3107-3116

[8] Yip CK: The Role of Calcium in Geopolymerisation. PhD Thesis, The University of Melbourne, Department of Chemical Engineering, Melbourne, Australia, 2004

[9] P. Duxon et al: Geopolymer technology: the current state of the art, J Mater Sci., Vol.42, 2007, pp.2917-2933

[10] S. Mallicoat et al: Novel alkali-bonded ceramic filtration membranes, Ceramic Engineering and Science Proceedings, Vol.26, 2005, pp.26-37

[11] J. Davidovits: Properties of Geopolymer Cements, First International Conference on Alkaline Cements and Concrete, Scientific Research Institute on Binders and Materials, Vol.1, Kiev State Technical University, Kiev, Ukraine, 1994, pp.131-149

[12] S. D. Wang et al: Hydration products of alkali activated slag cement, Cement and Concrete Research, Vol.25, 1995, pp.567-571

[13] I. G. Richardson et al: The characterization of hardened alkali-activated blast-furnace slag paste and the nature of the calcium silicate hydrate (C-S-H), Cement and Concrete Research, Vol.24, 1994, pp.813-829

[14] S. Song et al: Pore solution of alkali-activated ground granulated blast-furnace slag, Cement and Concrete Research, Vol.29, 1999, pp.159-170

[15] J.I. Escalante-Garcia et al: Hydration products and reactivity of blastfurnace slag activated by various alkalis, J. Am. Ceram. Soc., 2003, pp.2148-2153

[16] P.J. Shilling et al: Microstructure, strength and reaction products of ground granulated blast-furnace slag activated by highly concentrated NaOH solution, J. Mater. Res. Vol.91, 1994, pp.188-197